



HAL
open science

Vegetation cover at the water surface best explains seed retention in open channels

Gabrielle Rudi, Gilles Belaud, Sébastien Troiano, Jean-Stéphane Bailly,
Fabrice Vinatier

► **To cite this version:**

Gabrielle Rudi, Gilles Belaud, Sébastien Troiano, Jean-Stéphane Bailly, Fabrice Vinatier. Vegetation cover at the water surface best explains seed retention in open channels. *Ecohydrology*, 2021, 14 (2), pp.e2263. 10.1002/eco.2263 . hal-03138616

HAL Id: hal-03138616

<https://hal.inrae.fr/hal-03138616>

Submitted on 7 Jun 2021

HAL is a multi-disciplinary open access archive for the deposit and dissemination of scientific research documents, whether they are published or not. The documents may come from teaching and research institutions in France or abroad, or from public or private research centers.

L'archive ouverte pluridisciplinaire **HAL**, est destinée au dépôt et à la diffusion de documents scientifiques de niveau recherche, publiés ou non, émanant des établissements d'enseignement et de recherche français ou étrangers, des laboratoires publics ou privés.

1
2
3
4
5
6
7
8
9
10
11
12
13
14
15
16
17
18
19
20
21
22
23
24
25
26
27
28
29
30
31
32
33
34
35

Title: Vegetation cover at the water surface best explains seed retention in open channels

Short title: Vegetation cover at the water surface best explains seed retention

Authors : Gabrielle RUDI^{a*}, Gilles BELAUD^b, Sébastien TROIANO^a, Jean-Stéphane BAILLY^{ac},
Fabrice VINATIER^a

^a LISAH, Univ Montpellier, INRAE, Institut Agro, IRD, Montpellier, France
^b G-Eau, Univ Montpellier, AgroParisTech, CIRAD, INRAE, Institut Agro, IRD,
Montpellier, France
^c AgroParisTech, 75005, Paris, France

* Corresponding author – 2 place Pierre Viala, 34060 Montpellier, France
gabrielle.rudi@gmail.com

ABSTRACT

Hydrochorous dispersal through agricultural channels plays a role in structuring plant communities across agricultural landscapes. To date, research on seed retention in vegetated areas has mainly focused on vegetation types with simple architecture (often cylinders), which consequently do not represent real vegetation features. Here, we test the hypothesis that vegetation cover estimated at the water surface best explains floating seed retention in open channels. We therefore proposed an experiment to measure seed retention in a controlled environment across a large range of hydraulic conditions and vegetation architecture types. We used three types of artificial plants with contrasting morphotypes, and real seeds of *Rumex crispus*. Vegetation metrics were calculated on the basis of 3D plant models. We also tested the additivity of seed retention as a function of the length of vegetated area crossed by the seeds. We developed a semi-empirical formula for predicting seed retention. The main results of the experiment show that (i) the seed retention rate reacts differently to changes in density according to species (ii) vegetation cover at the free water surface, potentially in contact with seeds, is a generic predictor of floating seed retention whatever the nature of the vegetated cover (iii) 95% of seed retention was reached for a large range of surface vegetation ratios and length of vegetation cover. The proposed formula could be used by

36 stakeholders (farmers and ecologists) to estimate the amount of vegetation needed in a channel to
37 limit or enhance seed dispersal.

38

39 **Keywords (max 8): Vegetated channel; Agricultural drainage networks; Propagule dispersal;**
40 **Vegetation porosity; Vegetation metrics; Hydrochory; *Rumex crispus*; 3D plant model**

41

42 **1. INTRODUCTION**

43

44 Hydrochorous dispersal plays a major role in structuring vegetation communities (Gurnell et al.,
45 2006; Nilsson et al., 1991, 2010; Ridley, 1930). In agricultural areas, some plant species are able to
46 travel hundreds of metres via semi-natural waterways, such as ditches or irrigation channels (Rudi
47 et al., 2018; Soomers et al., 2010; van Dijk et al., 2014). Plant dispersal can therefore be favoured
48 by a network-like organization of waterways, and propagules can readily travel through the
49 agricultural landscape, either causing economic losses for farmers when the propagules compete
50 with their crops (Petit et al., 2011), or contributing to the maintenance of community species
51 richness and increasing genetic diversity in populations (Nilsson et al., 2010). Plant richness in
52 agricultural channels provides numerous microhabitat types and contributes to the connection of
53 populations of mobile organisms, including amphibians, mammals and insects, which would
54 otherwise be isolated in intensively cropped areas (Dollinger et al., 2015).

55

56 The interplay between propagule features, hydrodynamic characteristics and waterway properties
57 drives propagule dispersal (Greet et al., 2011, 2012; Hyslop and Trowsdale, 2012). The propagules'
58 features, especially those determining the duration of buoyancy (Boedeltje et al., 2003; Carthey et
59 al., 2016; Riis and Sand Jensen, 2006), are important factors for explaining the distance of
60 transportation by water in natural ecosystems. The ability to float is mostly linked with the features
61 of the propagules, such as density, size and shape. For floating propagules, the mean flow velocity
62 (Defina and Peruzzo, 2010) and turbulent diffusion (White and Nepf, 2003) as well as
63 hydrodynamic conditions at the water surface, can be related to the rates of deposition in the
64 channels (Merritt and Wohl, 2002). Other retention factors include the presence and abundance of
65 vegetation (Chambert and James, 2009; Cornacchia et al 2019, Defina and Peruzzo, 2010; Liu et al
66 2019; Peruzzo et al. 2012, 2016), and vegetation type (Jager et al., 2019), especially in narrow
67 agricultural waterways, such as channels and ditches (Rudi et al., 2018; Rudi et al., 2020; Soomers
68 et al., 2010).

69

70 At the local scale, Defina and Peruzzo (2010) describe two mechanisms for temporary trapping of
71 propagules in emergent vegetation: (i) wake trapping, in which the propagules are retained in the
72 recirculation zone behind a plant (White and Nepf, 2003), and (ii) inertial impaction, in which the
73 inertia of a propagule allows it to escape from the streamline and meet a stem (Palmer et al., 2004);
74 and two possible mechanisms of permanent trapping: (i) net trapping, in which a bunch of stems or
75 leaves forms a net-like structure, and (ii) the "Cheerios effect" (Vella and Mahadeven, 2005), which
76 is explained by the deformation of the water surface linked with surface tension. For permanent
77 propagule retention, note that the Cheerios effect is significant when the spacing between stems is
78 greater than the propagule size and in slow-flowing conditions (Chambert and James, 2009). Some
79 semi-empirical models have been developed to characterize propagule retention distances in
80 vegetated media relying on channel experiments (Defina and Peruzzo, 2010; Liu et al 2019;
81 Peruzzo et al., 2012, 2016). These models have been mainly developed for slow flowing water and
82 low to medium vegetation densities and focused mainly on the Cheerios effect. They described the
83 probability of interaction and capture of propagules in vegetation. As described by Defina and
84 Peruzzo (2012), the probability that a propagule reaches a specific distance depends on the
85 propagule mean path length before permanent capture, the probability of interaction, the probability
86 of permanent capture, and the mean centre-to-centre spacing between stems. In these experiments,
87 the vegetation has usually been represented with rigid arrays, except in Defina and Peruzzo (2010,
88 2012), who used flexible plastic plants. The vegetation metrics used in the developed models are the
89 mean centre-to-centre distance between stems, the mean spacing between adjacent cylinders (taking
90 into account the stem diameter), and the density of plants (Defina and Peruzzo, 2010, 2012; Liu et
91 al. 2019, Peruzzo et al. 2012, 2016).

92
93 However, in field conditions, complex vegetation patterns are frequently observed. Vegetation
94 exhibits a vertical variability, and consequently, the area of vegetation at the water surface that can
95 potentially interact with propagules varies with the fluctuations in the water level. There is currently
96 a lack of vegetation metrics and semi-empirical generic formulas able to predict the rates of
97 propagule retention in the large range of hydrodynamic conditions observed in the field. Some
98 attempts have been made to measure the percentage of plant cover at the water surface (Rudi et al.,
99 2018) or the plant cover "porosity" (Vinatier et al., 2018) for real plant covers to characterize
100 patterns of propagule deposition along agricultural channels. In these experiments, the tallest layers
101 of vegetation hid the vegetation at the water surface and made it difficult to reconstruct the patterns
102 of vegetation cover at the water surface. Moreover, as pointed out by Green (2005), the vertical
103 heterogeneity of the vegetation profile needs to be taken into account in studies focusing on
104 interactions between vegetation and fluxes of matter. Testing the importance of the specific

105 vegetation surface permeability to propagules against other traditional metrics describing the
106 vegetation cover seems necessary for a better comprehension of hydrochory.

107

108 The study was motivated by questions on the retention ability of terrestrial and semi-aquatic
109 vegetation growing in agricultural channels and ditches in Mediterranean areas. One of the
110 specificities of these patches is that they generally cover the total width of the channels, and form a
111 relatively homogeneous cover. As will be detailed below, the experimental set-up therefore reflects
112 the conditions commonly observed in these systems.

113

114 In this study, floating seed retention in vegetated channels is investigated, focusing on a large range
115 of plant densities for three different types of emergent vegetation with complex architectures,
116 representative of the types of vegetation that can be found in agricultural drainage or irrigation
117 channels with medium velocity flow conditions. We hypothesized that vegetation cover estimated
118 for the fine layer constituting the water flow surface is the best predictor of seed retention compared
119 to other vegetation metrics. The specific purpose of the study was (i) to investigate seed retention
120 rates in various artificial plant covers that closely reproduce the plant covers observed in the field,
121 (ii) to test the hypothesis of additivity of seed retention according to the length of the vegetated
122 area, and (iii) to establish a semi-empirical retention function based on two components depending
123 on plant metrics and hydrodynamic conditions to test the relevance of the vegetation cover at the
124 surface to explain seed retention.

125

126 **2. MATERIALS AND METHODS**

127

128 **2.1. Experimental channel design**

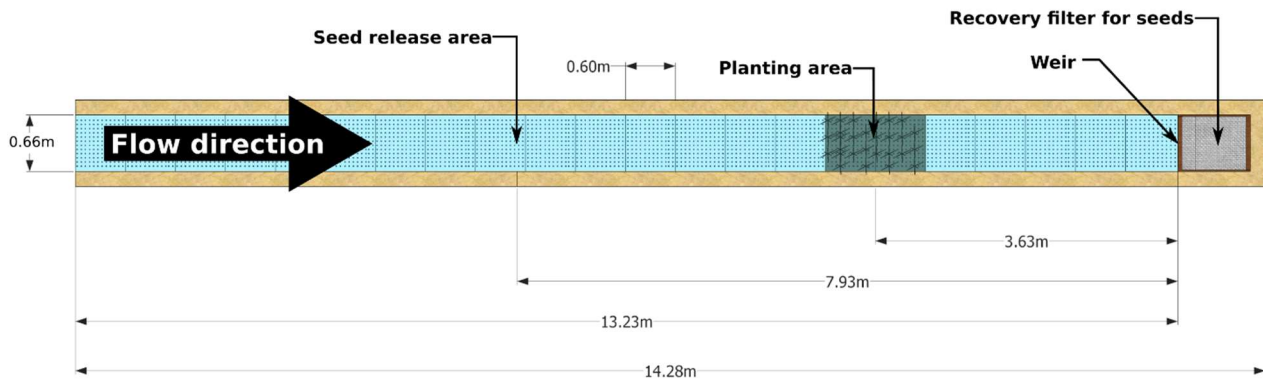
129

130 The experiments were conducted in controlled hydraulic conditions in an experimental cement
131 channel located at the Institut Agro – Montpellier SupAgro (Montpellier, France). The channel is
132 rectangular (9 m long and 0.66 m wide) (**Figure 1**). The slope is 0.0013 m/m. This channel was
133 chosen because its dimensions were consistent with those of the channels and ditches found in
134 southern France and with the morphologies of those channels, in which flows are generally
135 subcritical and turbulent. Commonly observed Froude and Reynolds numbers of these systems
136 could be reproduced in the channel. The water inflow was regulated thanks to a control structure
137 (constant level gate followed by baffle module weirs) ensuring a constant discharge ($\pm 5\%$). Then, a
138 flow tranquilizer followed by a 5-metre reach ensured the formation of a well-established flow
139 upstream of the channel. The downstream water level was controlled by a rectangular weir with a

140 sill of 10 cm. At the end of the channel, a net was placed to collect seeds. The water was then
141 filtered and recycled through the closed system.

142

143 **Figure 1: Schematic representation of the experimental channel.**



144

145

146 The selected steady-state flow rates varied from 10 L.s⁻¹ to 40 L.s⁻¹, determined with an accuracy of
147 +5% (Vinatier et al., 2017). The range of variation in the discharges is based on the heights of the
148 plants, in such a way that plants are never submerged.

149

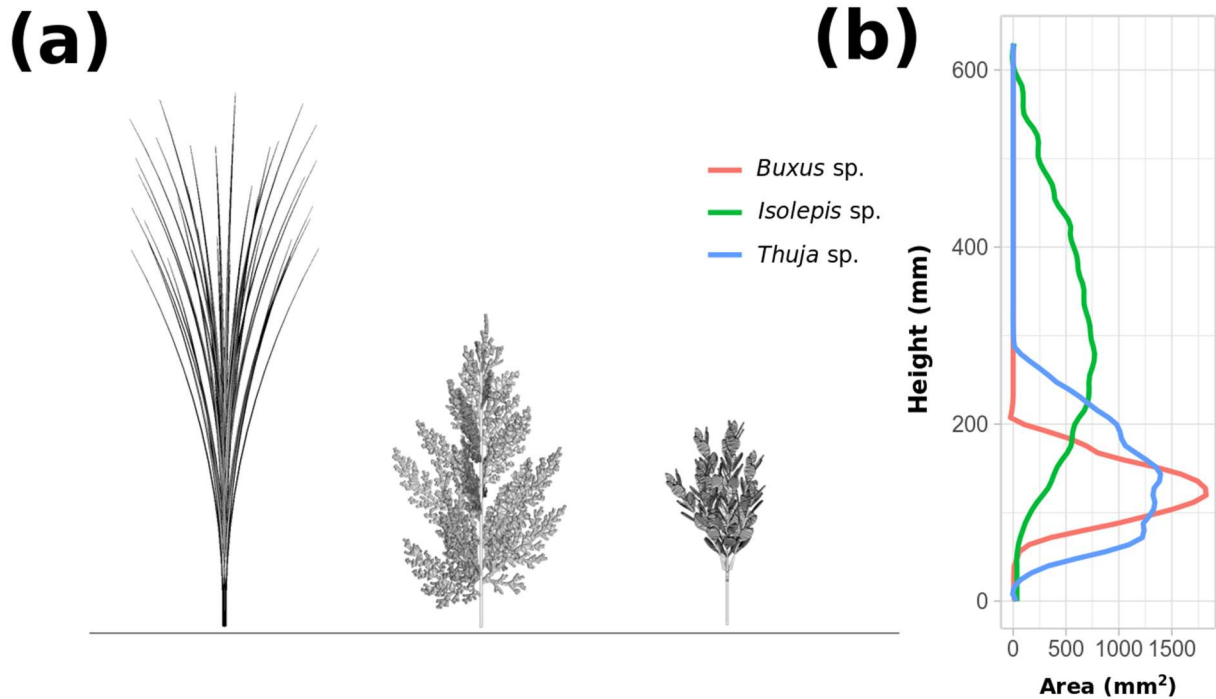
150 2.2 Plant material and its spatial arrangement

151

152 Three types of plastic plants of different architectures were chosen for the experiment: a Cyperaceae
153 (*Isolepis* sp.), a Cupressaceae (*Thuja* sp.) and a Buxaceae (*Buxus* sp.)
154 (<https://www.artificielles.com>) (Figure 2). We chose these types of plants because they represented
155 a diversity of architectural topologies characteristic of the plant diversity found in intermittent
156 agricultural channels. The Cyperaceae morphotype represented by *Isolepis* sp. (thin and elongated)
157 is similar to the grasses frequently encountered in channel banks, colonizing an intermediate
158 ecological niche between terrestrial and wetland environments. The Cupressaceae morphotype
159 (*Thuja* sp.) is characteristic of shrubby vegetation encountered in less well-managed channels. The
160 Buxaceae morphotype (*Buxus* sp.) is similar to that of some Asteraceae found in the bottoms of
161 channels, with a specific architecture consisting of a long stem surmounted by a vegetative spike.
162 **Table 1** presents the diversity of morphological characteristics of the studied artificial plants.

163

164 **Figure 2: (a) 2D representations of the three plants (*Isolepis* sp., *Thuja* sp. and *Buxus* sp., from**
165 **left to right) used for the experiment and (b) the vertical profile of their surface area**
166 **according to a horizontal plane.**
167



168
169
170
171 The plants were fixed on concrete panels (0.66*0.60 m) drilled with 144 holes, i.e., approximately
172 362 holes/m², filled with screw anchors to fix the plants. Fourteen densities were established in a
173 staggered pattern, representing the variability in natural plant densities found in ditches (Rudi, pers.
174 com). A picture of the vegetated area with a medium density (36 plants per concrete panel) from
175 above the channel for two panels is presented in **Figure 3**. The arrangement of plants in the channel
176 for all the density configurations is provided in **Appendix A**. Note that for all the density
177 configurations, the vegetation filled the channel width and was homogeneously distributed in the
178 channel.

179
180
181
182
183

184 **Figure 3: Picture of the vegetated area (*Isolepis* sp.) in the experimental channel (36 plants per**
185 **concrete panel on two panels).**



186

187

188

189 **2.3. Overview of the experiments**

190

191 Two seed release experiments were conducted in the experimental channel. The first experiment
192 aimed to characterize the retention rate of seeds in patches of vegetation with constant lengths (over
193 the length of two concrete panels, i.e., 1.2 m, with different plant density configurations, see **Table**
194 **2)** to assess the interactive effects of density per panel (D), species (SP) and discharge (Q) on seed
195 retention. In the second experiment, the same plant density was planted on one to eight panels (i.e.,
196 0.6 to 4.8 metres) to characterize the effect of the length of the patch (where NB is the number of
197 panels) on the seed retention and test the hypothesis of additivity of seed retention (**Table 2**). It is
198 important to note that for the second experiment, discharge and density were chosen to explore the
199 largest range of retention rates from one panel to 8 panels and differed for each species. A trial
200 without plants was conducted for each discharge tested in the experiment. Moreover, the results
201 from these two experiments were used to calibrate the developed model of seed retention based on
202 new vegetation metrics.

203

204

205

206

207 2.4 Seed release and counting

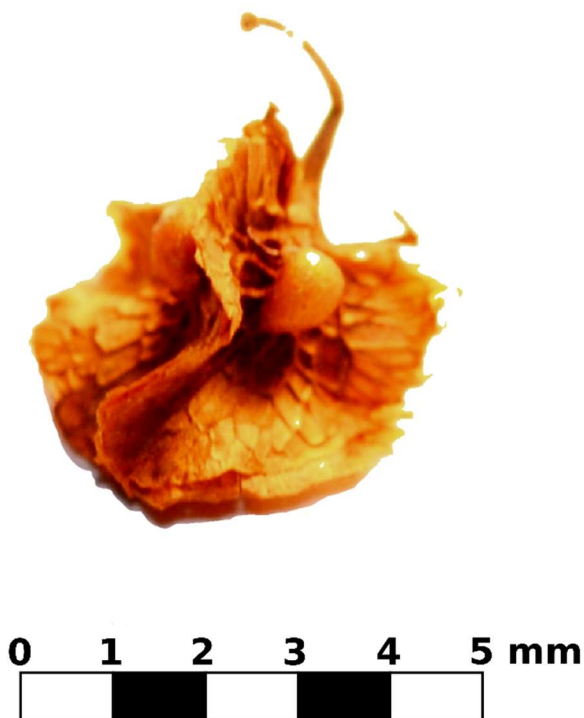
208

209 Seeds from curly dock (*Rumex crispus*) (**Figure 4**) were collected in Lattes (Hérault, France) in
210 October 2018. This weed was chosen because it is common in rural areas, and its seeds have the
211 potential to disperse via flow because they are contained in the calyx of the flower which has good
212 buoyancy (Uva et al., 1997). The buoyancy of the collected seeds was assessed by immersing 200
213 seeds in 10 pots of water (20 seeds per pot) for 5 days. This experiment showed that 100% of the
214 seeds were buoyant during the first 10 h of immersion (details of the experiment are provided in
215 **Appendix B**). This was consistent with the results of Cavers and Harper (1964) and Favre-Bac et al.
216 (2017), who classified *R. crispus* seeds as having long-term buoyancy compared to other species.
217 The weight of the seeds (5.35 mg (+/- 0.68 mg)) was estimated from the measurement of 10 lots of
218 10 seeds with a high-precision scale (Precisa XB 160M; precision: 0.001 g; accuracy: 0.01 g). The
219 seed diameter was measured as the average of 50 seeds (4.96 mm (+/- 0.76), including the calyx)
220 with a calliper.

221

222 **Figure 4: Picture of a curly dock (*Rumex crispus*) seed**

223



224

225

226 During the experiment, following the Eulerian framework described in Defina and Peruzzo (2010),
227 lots of 50 seeds were released at the head of the channel in the seed release area using a 60 cm-long
228 piece of metal. The lots were distributed homogeneously using this piece of metal, which covered
229 the width of the channel. For each release, we counted the seeds that travelled to the end of the
230 channel after a defined amount of time, depending on the length of the patch and the water
231 discharge. The retention rate of seeds was calculated according to the following formula:

232

$$233 \quad R_r(x) = \frac{N_{release} - N_{out}}{N_{release}} \quad \text{Equation 1}$$

234

235 where $R_r(x)$ is the retention rate over a vegetated distance of x metres, $N_{release}$ is the number of
236 seeds in each release (50 for this experiment) and N_{out} is the number of seeds reaching the tail end
237 of the experimental channel. Each release was repeated three times for one set of Q, SP and D.

238

239 Following Defina and Peruzzo (2010), we estimated that seeds were permanently trapped after a
240 period equal to one order of magnitude above the mean travel time of a seed for the whole test
241 section. For the first experiment (with two vegetated panels), this period was set at 2 min and 1 min
242 30 s for discharges equal to 10 L.s⁻¹ and above 10 L.s⁻¹, respectively, which is in accordance with
243 the period of 2 min set in Cornacchia et al. (2019), and with preliminary tests showing that there
244 was no seed release once these time limits were exceeded. For the second experiment, we adapted
245 the period to the number of vegetated panels, by multiplying the length of the period according to
246 the total number of vegetated panels, based on the periods chosen for two vegetated panels. For
247 each release, when the time elapsed, we collected all the seeds trapped in the patch of vegetation
248 before the next release. In total, 264 releases of 50 seeds were made in the first experiment and 111
249 in the second experiment, representing 18750 released seeds in total.

250

251 **2.5. Characterization of the seed retention rates relative to the experimental variables**

252

253 The effects of the experimental variables and their interactions on the R_r were analysed using a
254 binomial generalized linear model with logit link function (analysis of deviance with binomial
255 error). The experimental variables were Q, D, SP, and NB. The significance of each variable was
256 assessed via the change in deviance between the models with and without the variable.
257 Overdispersion was accounted for using quasi-binomial instead of binomial models.

258

259 For each combination of SP x Q for the first experiment (2 panels, corresponding to a distance of
260 1.20 metres), a sigmoid curve with the form

$$261 \quad R_r(1.2) = \frac{1}{1+e^{(-slope \times (D-D_{50}))}} \quad \text{Equation 2}$$

262 is fitted using the nonlinear least squares method to obtain D_{50} (the density needed to reach 50%
263 seed retention) and the slope of the linear relation between D and R_r .

264

265 **2.6. Characterization of the vegetation metrics**

266

267 Among the different metrics describing the influence of vegetation on ecohydrological processes
268 are the proportion of surface area containing vegetation (Green, 2005), the percentage of submerged
269 or emergent vegetation (Rudi et al., 2018), and the porosity of the vertical section of a channel
270 induced by vegetation (Vinatier et al., 2018); we reviewed all of these metrics to test the hypothesis
271 that vegetation at the water surface is the best predictor of seed retention.

272

273 Because of the complexity of the architecture of individual plants, there are no simple
274 measurements of the vegetation cover metrics, especially for the vegetation area in the thin slice
275 corresponding to the water surface that can potentially interact with the floating seeds.
276 Consequently, we constructed a three-dimensional model of each of the three artificial plants. This
277 was made possible because of the homogeneity of the artificial plants and their repetitive elements.

278

279 A 3D model of each plant was realized by first establishing a master of all plant attributes. Each leaf
280 of the artificial plant has been cut, numbered and scanned using a professional scanner (600 dpi
281 resolution). Leaf thickness, stem diameters and spacing between the different stem portions were
282 measured using a calliper. Orientations of leaves and stems were measured using a protractor. Then,
283 meshes of all plant attributes were assembled using CloudCompare software (Girardeau-Montaut
284 2014) to produce a continuous mesh for each plant.

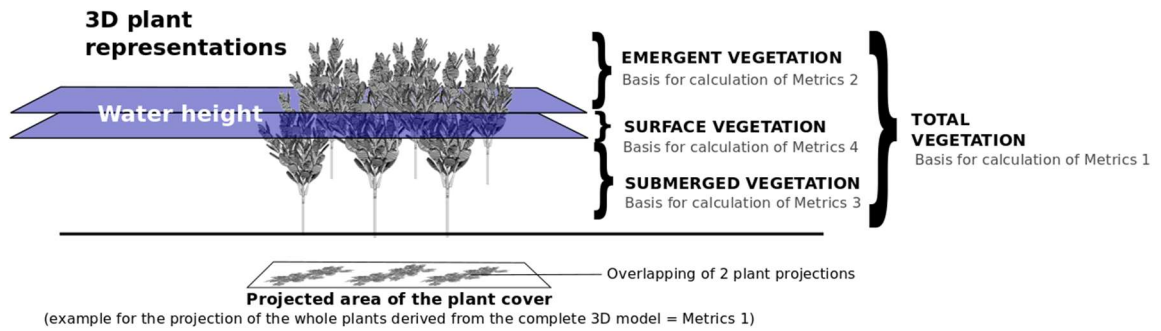
285

286 After this step, different vegetation metrics were derived from the projection of the 3D plants on the
287 horizontal plane of the channel (**Figure 5**):

- 288 • the projection of the whole plants on a horizontal plane, derived from the complete 3D
289 model (basis for calculation of Metrics 1),
- 290 • the projected areas of the emergent and submerged vegetation (emergent and submerged
291 vegetation on **Figure 5**) on a horizontal plane, derived from the model cropped by a plane at
292 the level of the water surface (basis for calculation of Metrics 2 and 3), and

- the area of the plant at the free surface of the water derived from the model sliced by two planes at 1 mm above and below the water level (basis for calculation of Metrics 4) (surface vegetation on **Figure 5**).

Figure 5: Illustration of the different types of vegetation metrics for a group representing the plant arrangement for a given density.



300

301

302

303 The different areas were calculated from (i) the product of each individual projected area by plant
 304 density for each experiment (“product” method) and (ii) a scene representing the 3D models
 305 arranged according to the spatial patterns found for each density (“scene” method). By construction,
 306 the overlapping surfaces of the high-density projections were summed in the “product” method and
 307 were merged in the “scene” method.

308

309 Then, we calculated the ratio of occupation of each vegetated area by dividing the area occupied by
 310 vegetation by the total planting area of the channel (on a horizontal plane) to obtain the four
 311 vegetation metrics, called $Metrics_{veg}$.

312

313

314 2.7. Characterization of hydrodynamics

315

316 The literature survey suggests that the hydrodynamic conditions at the water surface, and especially
 317 the velocity at the water surface, largely influence the retention rates. More specifically, seeds are
 318 transported with the current, and we expect their probability to pass the vegetation filter to increase
 319 with turbulence. Therefore, we introduced the non-dimensional Reynolds number, \mathfrak{R} , to
 320 characterize the nature of the flow patterns:

321

322

$$\Re = U \times H / \nu \quad \text{Equation 3}$$

323

324 where U corresponds to the average velocity over a section in $\text{m}\cdot\text{s}^{-1}$ ($U=Q/(B*H)$), H is the water
 325 height in m (corresponding to the characteristic length), B the width of the experimental channel in
 326 m, and ν is the kinematic viscosity in $\text{m}^2\cdot\text{s}^{-1}$. Weakly turbulent flows (low Reynolds number) should
 327 result in high retention rates ($R_r \rightarrow 1$) (in this case, surface tension will facilitate the capture by
 328 vegetation stems), while highly turbulent flows (large \Re) should result in low seed retention
 329 ($R_r \rightarrow 0$). The range of the Reynolds numbers in our experiments was assessed between 15000 and
 330 60000.

331

332 2.8. The additivity effect

333

334 Based on a constant probability of capture on each panel, we tested the additivity of our model
 335 based on the following formula:

336

$$R_r(x) = 1 - (1 - \widehat{R}_r(1.2))^{\left(\frac{x}{l}\right)} \quad \text{Equation 4}$$

337

338 where x is the vegetated distance travelled by the seeds (in metres), $\widehat{R}_r(1.2)$ is the mean
 339 experimental retention value for two vegetated panels, and l is the length of the two vegetated
 340 panels, i.e., 1.2 metres.

341

342 2.9. The generic formula for seed retention

343

344 The relation linking R_r to $Metrics_{veg}$ and \Re could be approximated by an exponential model of the
 345 form:

$$R_r(1.2) = 1 - e^{\left(\frac{-Metrics_{veg}}{a \times \Re \times 10^{-5}}\right)} \quad \text{Equation 5}$$

346

347 where a is a dimensionless parameter to estimate. The mathematical form respects the expected
 348 trends between R_r and \Re .

349

350 Combining **Equation 4** and **Equation 5**, we obtained the generic formula for seed retention:

351

$$R_r(x) = 1 - e^{\left(\frac{-Metrics_{veg} \times x}{a \times \Re \times 10^{-5} \times l}\right)} \quad \text{Equation 6}$$

352

353 Based on **Equation 6**, we tested what vegetation metrics best explained the seed retention rate (R_r)
354 from the two experiments on the basis of the R^2 and the RMSE between the estimated and observed
355 $\widehat{R}_r(1.2)$.

356

357 **2.10. Softwares**

358

359 All the statistical analyses were performed using R software (R Core Team, 2017). The processing
360 of the 3D models was performed using dedicated R packages (Rvcg, Morpho and data.table).

361

362 **3. RESULTS**

363

364 **3.1 Effect of density, discharge and type of species on seed capture**

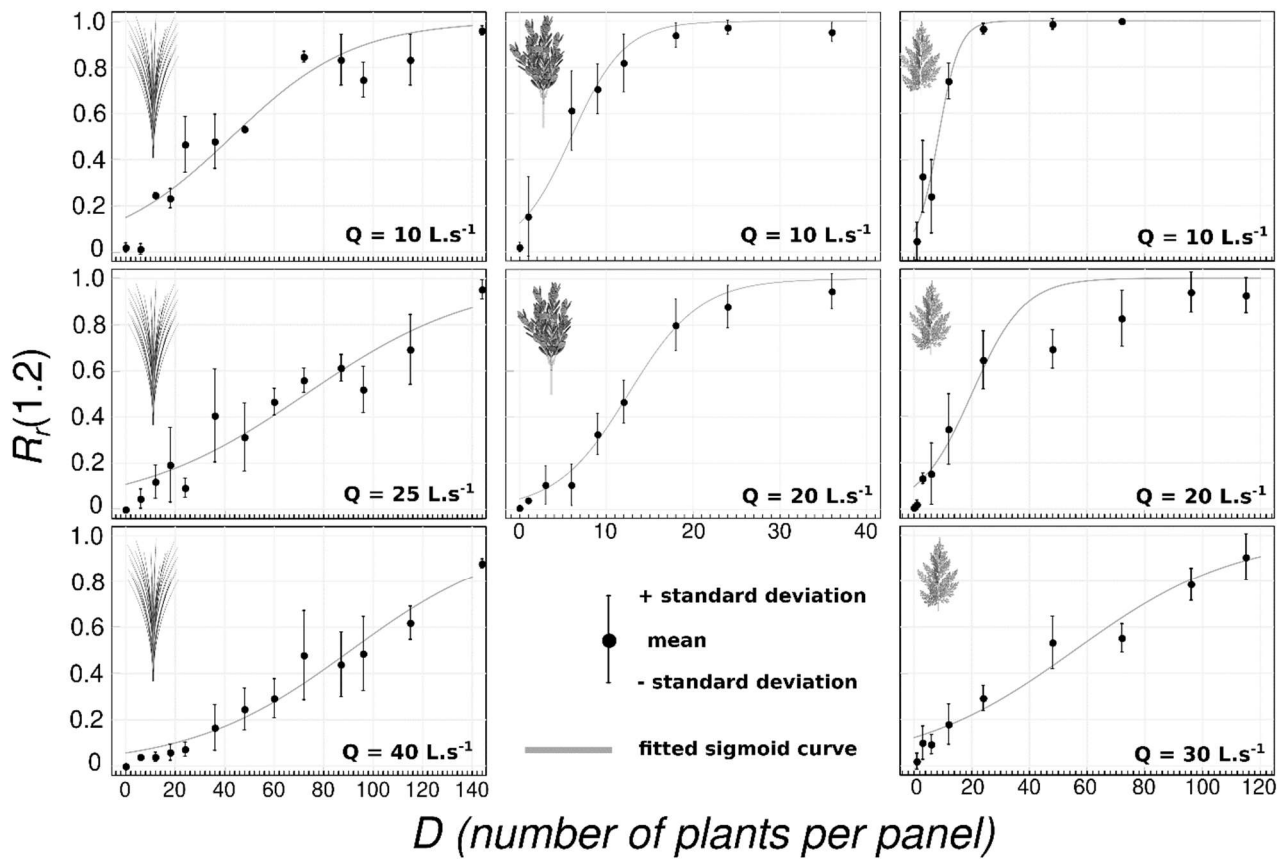
365

366 The results of the statistical analysis (**Table 3**) show that the discharge, density or type of species
367 significantly affects the rate of seed retention. The significant interaction between density and
368 species means that the seed capture rate react differently to changes in density according to species.

369 The results for the retention curves, as functions of plant density for each type of studied plant, are
370 presented in **Figure 6**. Fitted parameters are presented in **Table 4**.

371

372 **Figure 6: Seed capture rates R_r as a function of plant density D (number of plants by panel)**
373 **for *Isolepis* sp. (first column), *Buxus* sp. (second column), and *Thuja* sp. (third column).** The
374 solid line represents a sigmoid curve fitted using the nonlinear least squares method for each
375 combination of SP and Q. Fitted parameters are given in **Table 4**.



376

377

378

379 3.2. Additivity of the seed capture rate as a function of vegetation patch length

380

381 We first tested the significance of the influence of the number of vegetated panels on water height.
 382 We found that in the conditions of the study, the number of panels had a non-significant influence
 383 on water height (p-value = 0.123). This could be explained by the low density values tested for
 384 additivity (therefore, the vegetation did not significantly affect the hydraulic resistance).
 385 Consequently, we could neglect this effect in our experimental conditions.

386

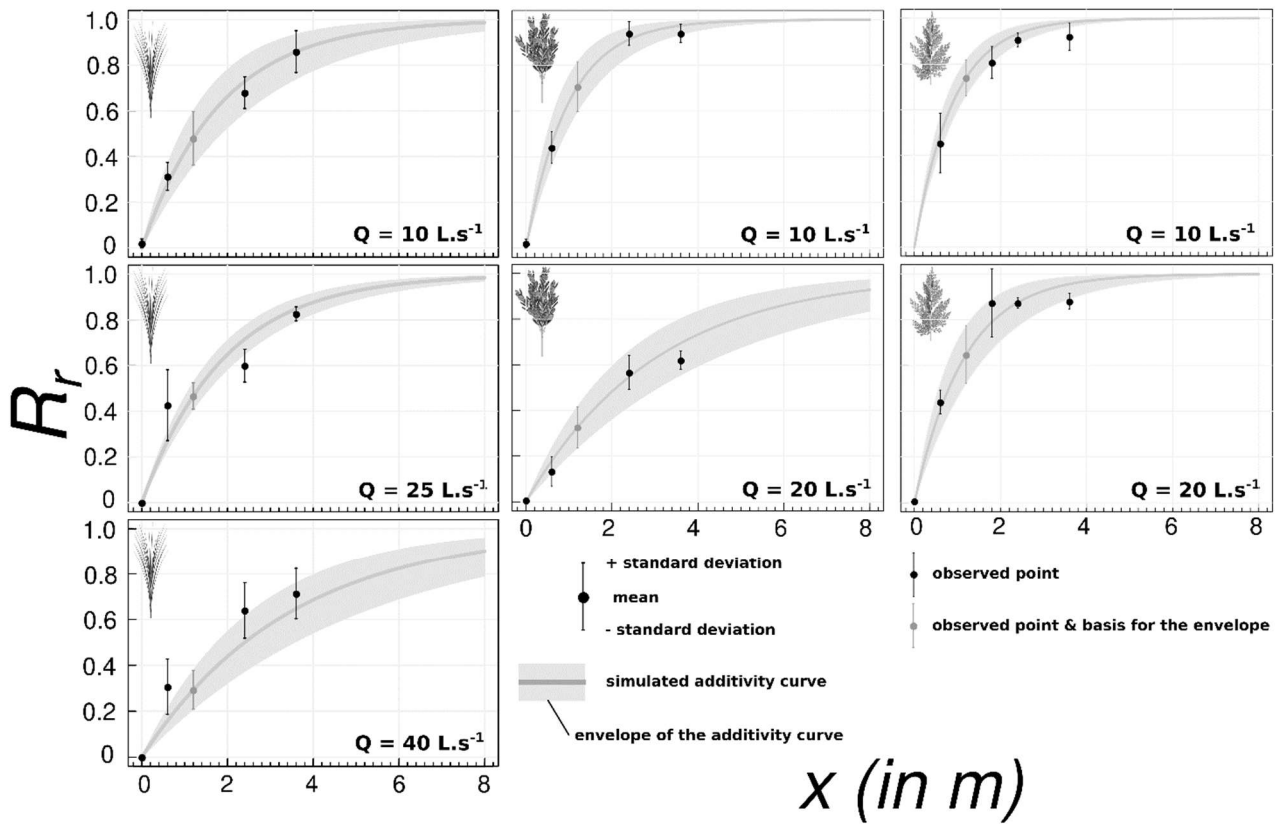
387 The envelope of the additivity curve, extrapolated from the standard error of the $\widehat{R}_r(1.2)$, generally
 388 encompasses the observed points for 1, 4, 6 and 8 panels (**Figure 7**). The global R^2 of the proposed
 389 model is 0.77 (+/-0.16).

390

391

392 **Figure 7: Comparison between the observed seed capture rates and predicted capture rates**
 393 **based on the additivity formula for the three plants (*Isolepis* sp. (first column), *Buxus* sp.**
 394 **(second column), and *Thuja* sp. (third column)). The mean and standard deviation (black points**
 395 **and arrays) values were calculated on the 3 repetitions of seed release experiment. The grey point**

396 and array is the mean and standard deviation for two vegetated panels, which served as a base for
 397 the calculation of the envelope (light grey).
 398



399

400

401

402 3.3. A generic formula for floating seed capture in differentiated plant covers

403

404 The calculated surface vegetation ratio was between approximately two-fold and ten-fold lower
 405 than the whole, submerged and emergent vegetation ratios. The Pearson cross product correlation
 406 test was significant between vegetation metrics ($p < 0.001$). However, the correlation is low
 407 ($0.2 < \text{cor} < 0.6$) between surface vegetation and the other metrics, and higher ($\text{cor} > 0.6$) when
 408 comparing the metrics calculated by summing individual areas with the metrics calculated from a
 409 scene (**Figure 5**). The metrics calculated from the “product” method exceeded the total area of the
 410 channel, especially for the whole and emergent vegetation of *Isolepis* sp., due to the high degree of
 411 overlap observed for this species.

412

413 As shown in **Table 5**, the use of the surface vegetation ratio (Metrics 4) led to the best results
 414 ($R^2=0.90$ and $\text{RMSE}=0.083$ for the “scene” method, and $R^2=0.58$ and $\text{RMSE}=0.178$ for the
 415 “product” method), regardless of how it was calculated. Considering a scene representing real

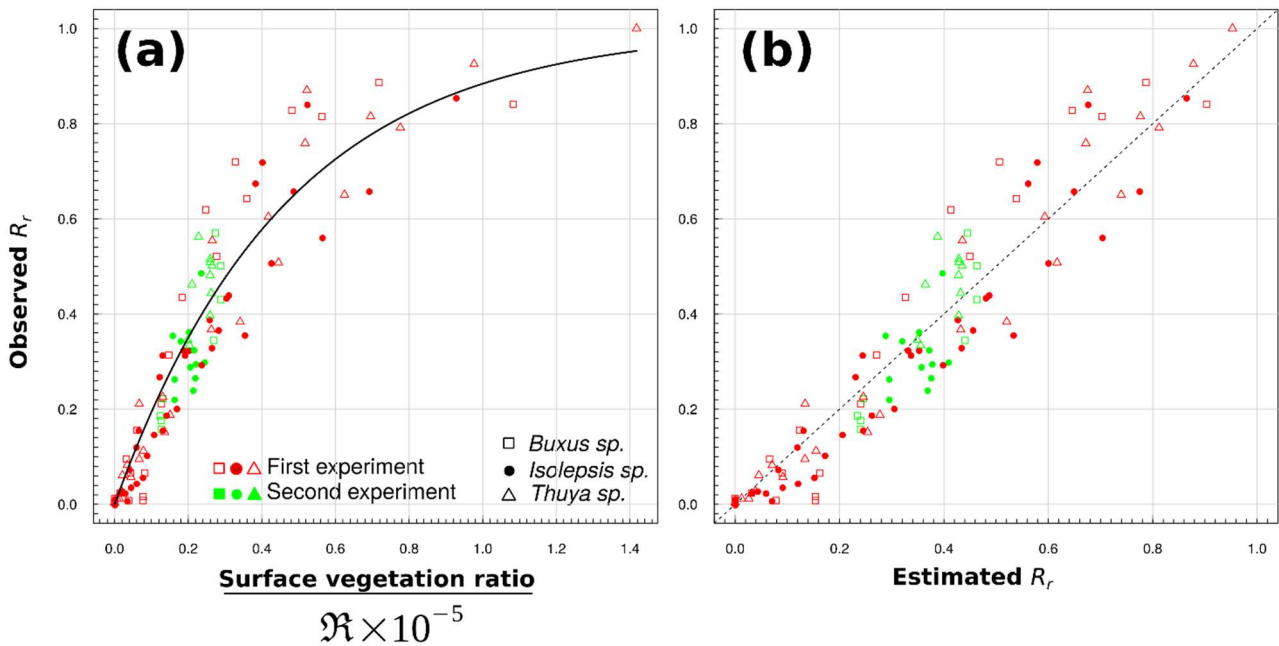
416 spatial arrangements instead of the product of each individual plant area by density increased the
 417 performance of the models. The metrics calculated for the total vegetation (Metrics 1) and the
 418 emergent vegetation (Metrics 2) led to the worst results ($R^2 < 0.30$ and $RMSE > 0.25$).

419
 420 Regarding the seed retention rate in the best model corresponding to the scene method and use of
 421 “Surface vegetation ratio” metrics (Metrics 4) ($R^2 = 0.90$ and $RMSE = 0.083$), **Figure 8** shows a
 422 homogeneous dispersion of the whole dataset across the fitted model. The data from the second
 423 experiment (additivity) were also included in the model, although they cover a lower range of
 424 vegetation metrics and hydraulic conditions. In **Table 6**, we observed that every studied plant was
 425 well fitted by the model.

426

427 **Figure 8: (a) Seed capture rate (R_r) as a function of the best combination of vegetation metrics**
 428 **and \mathfrak{R} . The solid line corresponds to the fit of the nonlinear model to the data. (b) Comparison**
 429 **between the observed and estimated R_r according to the model. The dashed line indicates a**
 430 **perfect fit between the observation and estimation.**

431



432

433

434

435

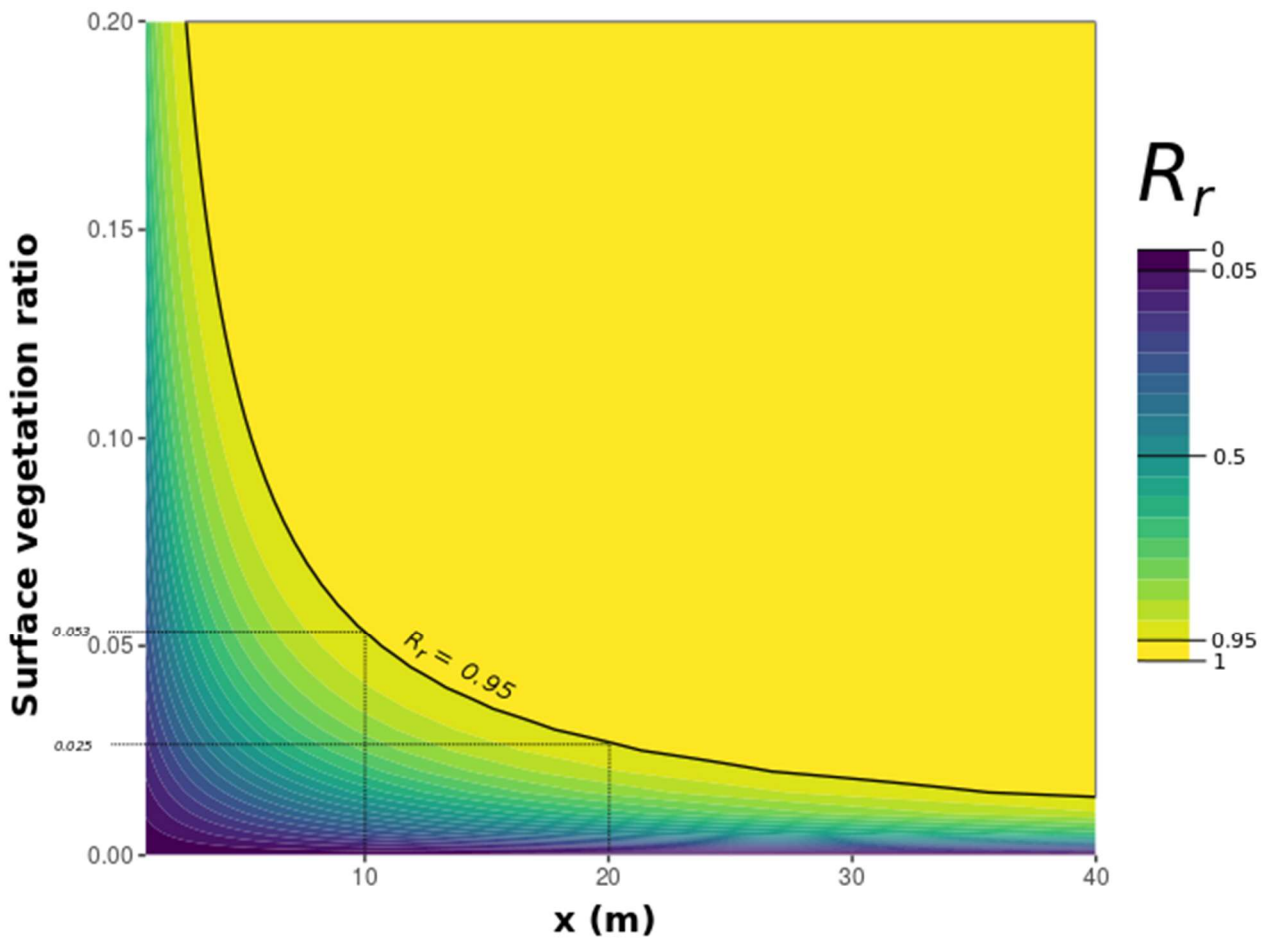
436

437

438

439 **Figure 9** indicates that 95% seed retention was reached for a large range of surface vegetation ratios
 440 and channel lengths (in hydrodynamic conditions allowing a Reynolds \Re of 32000). Basically, with
 441 an R_r isoline equal to 0.95, channels of 10 metres and 20 metres retained 95% of the seeds if the
 442 surface vegetation covered 5.3% and 2.5% of the water surface area, respectively.
 443

444 **Figure 9: Lattice plot based on the generic formula (Equation 6) and calibrated on the**
 445 **experimental data for a surface vegetation ratio between 0 and 20% and a channel length**
 446 **between 0 and 40 metres, with the \Re value being fixed in the formula at 32 000 (which can**
 447 **correspond, for example, to a water height of 15 cm and an average velocity of 0.21 m.s⁻¹)**



448
 449
 450
 451
 452
 453
 454
 455
 456

4. DISCUSSION

4.1. The area occupied by vegetation at the water surface is a relevant metric for seed retention prediction in a vegetated cover

457

458 This experiment showed the relevance of using the area occupied by vegetation at the water surface
459 instead of the area calculated from the total, emergent or submerged vegetation as a predictor of the
460 seed capture rate in a vegetated channel. The use of the area occupied by vegetation at the water
461 surface is interesting when focusing on plant covers with varied morphologies, because this metric
462 is generic and works for the three types of vegetation covers tested.

463

464 In the experiment, the variations of discharge affected more the retention rates for *Thuja sp.* and
465 *Buxus sp.* than for *Isolepis sp.* This is due to the fact that discharge affects directly water height in
466 the channel, and the first two species display a greater variability of surface area according to water
467 height than *Isolepis sp.* (see Figure 2b).

468

469 The additivity of the formula has been demonstrated on distances under 10 m with low vegetation
470 densities. Higher vegetation densities would exert a significant influence on hydraulic conditions,
471 especially height and velocity (Nepf, 2012), and the Reynolds number should be corrected as a
472 consequence.

473

474 Our results reinforce the idea that representing vegetation cover as a porous media is an efficient
475 approach for understanding water transport and particle transport in vegetated areas, as was
476 highlighted in recent works focused on interaction between water transport and vegetation (see
477 Rubol et al., 2018 and Vinatier et al., 2017 for example). However, in this experiment, the spatial
478 distribution of plants in the channel is relatively homogeneous. In configurations in which the
479 vegetation is heterogeneously distributed, preferential transfers are observed (Cornacchia et al.,
480 2019; Erktan et al., 2013; Nepf et al., 2012). Indeed, the phenomena of flow divergence at the patch
481 scale explain these preferential transfers, which could be susceptible to modifications in the
482 relationship between the area occupied by vegetation and seed capture.

483

484 **4.2. 3D representation of vegetation is an original and efficient method for characterizing** 485 **plant cover at the water surface**

486

487 The 3D representation of vegetation is an efficient approach, especially in contexts of high plant
488 density or when plants are largely above the water level; in the latter case, techniques using
489 photographs to reconstruct the area covered by vegetation from above have poor accuracy (because
490 of the effect of sheltering), as revealed by our results. In situations in which we possess 3D models
491 for each type of plant encountered in agricultural channels, we could represent any vegetated cover

492 and calculate the area at the water surface. Moreover, in the future, 3D plant models could help to
493 calculate more evolved vegetation metrics commonly used in landscape ecology, such as core area
494 or patch cohesion formed by the vegetation at the water surface.

495

496 However, the use of 3D plant models has limits. First, the production of 3D models is time
497 consuming for real plants, and it would be even more time consuming if we wanted to create
498 models for plants at different phenological stages. Moreover, in this study, the hydrodynamic
499 conditions did not significantly modify the plant structure. However, plant reconfiguration has been
500 observed under some hydrodynamic conditions (Vogel, 1996), and the degree of bending is usually
501 a function of water velocity (Chapman et al., 2015; Luhar and Nepf, 2011) and height. The 3D
502 models that we developed would be improved by being able to bend under flow drag forces. The
503 integration of computational fluid dynamic tools, such as OpenFOAM (www.openfoam.com) or
504 Fluent (www.ansys.com), could allow the creation of this type of bowed plant model, but the
505 amplitude of reconfiguration, the flex points and the representation of the streamlining of leaves as
506 a function of water velocity still need to be characterized by further studies.

507

508 It will be necessary to test the effect of seed characteristics in the context of the main processes
509 controlling vegetation and seed interactions. It has been shown that seed traits such as weight, size,
510 density and shape influence interactions with vegetation when the Cheerios effect is the major
511 mechanism of seed retention (Chambert and James, 2009; Liu et al., 2019; Peruzzo et al., 2016),
512 i.e., when the water velocity is slow and the spacing between the stems of the vegetation is greater
513 than the particle diameter (Chambert and James, 2009; Liu et al., 2019; Peruzzo et al., 2016). In our
514 hydrodynamic conditions, with net trapping being the major mechanism of seed capture, it is
515 possible that seed features also influenced the rate of seed retention in our experiment. For example,
516 de Jager et al. (2019) showed that large seeds were less affected by net-trapping than smaller ones.
517 The number of seeds released in the channel should also be considered. In our experiments, we
518 observed that seeds sometimes formed clusters (due to the Cheerios effect) more susceptible to
519 being captured by vegetation, especially when vegetation presented indented patterns, as for *Buxus*
520 sp. and *Thuja* sp.

521

522 **4.3. Implications for the agroecological management of agricultural channels**

523

524 It has been shown that agricultural channels could be significant dispersal vectors for weeds
525 because they allow seeds to travel hundreds of metres in a few hours (Rudi et al., 2018; Soomers et
526 al., 2010). From a practical point of view, the developed formula provided an indication of the

527 surface vegetation cover needed for a given channel length to reach a specified objective of retained
528 seed rate. For portions of ditches of 10 metres, it would be necessary to have a surface vegetation
529 ratio of 5.3% to retain 95% of seeds (with a Reynolds of 32 000, see Figure 9). Considering that the
530 surface vegetation ratio is between twice and ten times lower than the total vegetation ratio (see
531 §3.3), vegetation coverage of 53% in the channel ($5.3\% * 10$) should be sufficient to retain 95% of
532 the seeds transported by the channel. Previous studies of vegetation cover dynamics in agricultural
533 channels (Dollinger et al., 2017; Levavasseur et al., 2014) have revealed that management practices
534 were a lever to control vegetation cover in space and time, and we should then be able to control
535 hydrochorous seed dispersal through these management practices.

536

537 This work also confirms that water height variations, even moderate, play a role in the dispersal and
538 subsequent establishment of plants in agricultural waterways, as observed by Engström et al. (2009)
539 and Cornacchia et al. (2019) in other aquatic ecosystems. Consequently, in agricultural channels,
540 conserving a part of the vegetation that exceeds the maximal depth of the channel can guarantee
541 retention and limitation of dispersal. In this sense, tall plants (i.e., taller than 50 cm) can play a
542 preponderant role, because maximal depths in drainage channels and secondary/tertiary irrigation
543 channels are generally approximately 50 cm in the studied ecosystems.

544

545 The developed prediction formula for seed retention is rather easy to use and can serve to assess the
546 services of weed spreading limitation in agricultural landscapes or natural revegetation. Therefore,
547 it is well adapted to be integrated in studies assessing benches of ecosystem services provided by
548 vegetation of hydro-agricultural waterways such as ditches and channels (water transport regulation,
549 weed spreading limitation or enhancement, erosion limitation). Indeed, one of the drawbacks of
550 multifunctional studies is the need to choose between indicator-based approaches (such as biomass,
551 as a distant proxy for estimating the propagule retention capacity of vegetated channels), and
552 physical approaches (e.g., using advection-dispersion equations, which need parameterization and
553 substantial computing capacity and cannot be deployed when studying services on extended
554 networks of channels) (Rudi, 2019; Rudi et al., 2020). Therefore, the developed formula in this
555 research proposes a semi-empirical approach of medium complexity, process-based, to assess seed
556 retention in agricultural channels.

557

558 **5. CONCLUSION**

559

560 Seed dispersal by hydrochory through agricultural channels greatly influences weed spatio-temporal
561 distributions at the landscape scale. Natural vegetation growing in these channels plays a major role

562 in the retention rates of weed propagules, and these retention rates are greatly influenced by both
563 vegetation features and hydrodynamic conditions. This research focused on the characterization of
564 *R. crispus* seed capture rates in three different artificial vegetation covers (*Isolepis* sp., *Thuja* sp.,
565 and *Buxus* sp.) in an experimental channel. We compared the relevance of different vegetation
566 metrics and showed that the cover of vegetation at the water surface, calculated from 3D plants, was
567 the best predictor of seed capture. We proposed a generic and semi-empirical formula to predict the
568 seed capture rate in vegetated channels as a function of vegetation cover at the water surface and
569 hydrodynamic conditions. This research supports the idea that the use of 3D plant models is an
570 efficient way to understand water-plant-particle interactions in open channels. Our results have
571 practical implications for the agroecological management of agricultural channels because they can
572 inform on the relevant maintenance practices to manage vegetation according to the intended
573 objectives of weed spreading limitation or natural revegetation through agricultural networks.
574 Indeed, the choice between different options for vegetation management involves different
575 vegetation dynamics along the year in terms of density or height of the cover (Dollinger et al., 2017;
576 Levavasseur et al., 2014). The proposed formula could be used as a basis for a wide variety of
577 vegetation covers and extended to other types of floating seeds.

578 **ACKNOWLEDGEMENTS**

579

580 The authors would like to thank Cédric Guillemain and Fabien Roudil for their help during the
581 channel experiment. We would also like to thank first-year students from l'Institut Agro
582 (Montpellier SupAgro) engineering program (years 2017-2018 and 2018-2019) for performing the
583 preliminary trials with us. This work (ID 1702-008) was publicly funded through ANR (the French
584 National Research Agency) under the “Investissements d’avenir” programme with the reference
585 ANR-10-LABX-001-01 Labex Agro and coordinated by Agropolis Fondation under the frame of I-
586 SITE MUSE (ANR-16-IDEX-0006). Inputs from two anonymous reviewers greatly improved the
587 manuscript, and we are grateful for their recommendations.

588

589 **CONFLICT OF INTEREST**

590

591 No conflict of interest was declared.

592

593 **DATA AVAILABILITY STATEMENT**

594

595 The data that support the findings of the study will be available online (Rudi et al. 2020 -
596 <https://doi.org/10.5281/zenodo.3947814>) from the date of publication.

597

598

599 REFERENCES

600

601 Boedeltje, G., Bakker, J. P., & ter Heerdt, G. N. J. (2003). Potential role of propagule banks in the
602 development of aquatic vegetation in backwaters along navigation canals. *Aquatic Botany*, 77(1),
603 53–69. [https://doi.org/10.1016/S0304-3770\(03\)00078-0](https://doi.org/10.1016/S0304-3770(03)00078-0)

604

605 Carthey, A. J. R., Fryirs, K. A., Ralph, T. J., Bu, H., & Leishman, M. R. (2016). How seed traits
606 predict floating times : A biophysical process model for hydrochorous seed transport behaviour in
607 fluvial systems. *Freshwater Biology*, 61(1), 19–31. <https://doi.org/10.1111/fwb.12672>

608

609 Cavers, P. B., & Harper, J. L. (1964). Biological flora of British Isles. *Rumex obtusifolius* L. and *R.*
610 *crispus* L. *Journal of Ecology*, 52, 737-766.

611

612 Chambert, S., & James, C. S. (2009). Sorting of seeds by hydrochory. *River Research and*
613 *Applications*, 25(1), 48–61. <https://doi.org/10.1002/rra.1093>

614

615 Chapman, J. A., Wilson, B. N., & Gulliver, J. S. (2015). Drag force parameters of rigid and flexible
616 vegetal elements. *Water Resources Research*, 51(5), 3292–3302.
617 <https://doi.org/10.1002/2014WR015436>

618

619 Cornacchia, L., van der Wal, D., van de Koppel, J., Puijalon, S., Wharton, G., & Bouma, T. J.
620 (2019). Flow-divergence feedbacks control propagule retention by in-stream vegetation : The
621 importance of spatial patterns for facilitation. *Aquatic Sciences*, 81(1), 17.
622 <https://doi.org/10.1007/s00027-018-0612-1>

623

624 Defina, A., & Peruzzo, P. (2010). Floating particle trapping and diffusion in vegetated open channel
625 flow. *Water Resources Research*, 46(11), W11525. <https://doi.org/10.1029/2010WR009353>

626

627 Defina, A., & Peruzzo, P. (2012). Diffusion of floating particles in flow through emergent
628 vegetation : Further experimental investigation. *Water Resources Research*, 48(3).
629 <https://doi.org/10.1029/2011WR011147>

630

631 Dollinger, J., Dagès, C., Bailly, J.-S., Lagacherie, P., & Voltz, M. (2015). Managing ditches for
632 agroecological engineering of landscape. A review. *Agronomy for Sustainable Development*, 35(3),
633 999–1020. <https://doi.org/10.1007/s13593-015-0301-6>

634

635 Dollinger, J., Vinatier, F., Voltz, M., Dagès, C., and Bailly, J.-S. (2017). Impact of maintenance
636 operations on the seasonal evolution of ditch properties and functions. *Agricultural Water*
637 *Management*, 193, 191–204.

638

639 Engström, J., Nilsson, C., & Jansson, R. (2009). Effects of stream restoration on dispersal of plant
640 propagules. *Journal of Applied Ecology*, 46(2), 397-405.

641

642 Erktan, A., Cécillon, L., Roose, E., Frascaria-Lacoste, N., & Rey, F. (2013). Morphological
643 diversity of plant barriers does not increase sediment retention in eroded marly gullies under
644 ecological restoration. *Plant and Soil*, 370(1/2), 653-669. JSTOR.

645

646 Favre-Bac, L., Mony, C., Burel, F., Seimandi-Corda, G., & Ernoult, A. (2017). Connectivity drives
647 the functional diversity of plant dispersal traits in agricultural landscapes: The example of ditch
648 metacommunities. *Landscape Ecology*, 32(10), 2029–2040. [https://doi.org/10.1007/s10980-017-](https://doi.org/10.1007/s10980-017-0564-1)
649 [0564-1](https://doi.org/10.1007/s10980-017-0564-1)

650

651 Girardeau-Montaut, D. (2014). CloudCompare: 3D point cloud and mesh processing software.
652 Available online: <https://www.danielgm.net/cc/> (accessed on 1 October 2018).

653

654 Godin, C., & Caraglio, Y. (1998). A Multiscale Model of Plant Topological Structures. *Journal of*
655 *Theoretical Biology*, 191(1), 1-46. <https://doi.org/10.1006/jtbi.1997.0561>

656

657 Green, J. C. (2005). Comparison of blockage factors in modelling the resistance of channels
658 containing submerged macrophytes. *River Research and Applications*, 21(6), 671–686.
659 <https://doi.org/10.1002/rra.854>

660

661 Greet, J., Cousens, R. D., & Webb, J. A. (2012). Flow regulation affects temporal patterns of
662 riverine plant seed dispersal: Potential implications for plant recruitment. *Freshwater Biology*,
663 57(12), 2568-2579. <https://doi.org/10.1111/fwb.12028>

664

665 Greet, J., Webb, J. A., & Downes, B. J. (2011). Flow variability maintains the structure and
666 composition of in-channel riparian vegetation. *Freshwater Biology*, 56(12), 2514-2528.
667 <https://doi.org/10.1111/j.1365-2427.2011.02676.x>
668

669 Gurnell, A. M., Boitsidis, A. J., Thompson, K., & Clifford, N. J. (2006). Seed bank, seed dispersal
670 and vegetation cover: Colonization along a newly-created river channel. *Journal of Vegetation*
671 *Science*, 17(5), 665-674. <https://doi.org/10.1111/j.1654-1103.2006.tb02490.x>
672

673 Hyslop, J., & Trowsdale, S. (2012). A review of hydrochory (seed dispersal by water) with
674 implications for riparian rehabilitation. *Journal of Hydrology (New Zealand)*, 51(2), 137-152.
675

676 Jager, M. de, Kaphingst, B., Janse, E. L., Buisman, R., Rinzema, S. G. T., & Soons, M. B. (2019).
677 Seed size regulates plant dispersal distances in flowing water. *Journal of Ecology*, 107(1), 307-317.
678 <https://doi.org/10.1111/1365-2745.13054>
679

680 Levavasseur, F., Biarnès, A., Bailly, J. S., & Lagacherie, P. (2014). Time-varying impacts of
681 different management regimes on vegetation cover in agricultural ditches. *Agricultural Water*
682 *Management*, 140, 14–19. <https://doi.org/10.1016/j.agwat.2014.03.012>
683

684 Liu, X., Zeng, Y., & Huai, W. (2019). Floating seed dispersal in open channel flow with emergent
685 vegetation. *Ecohydrology*, 12(1), e2038. <https://doi.org/10.1002/eco.2038>
686

687 Luhar, M., & Nepf, H. M. (2011). Flow-induced reconfiguration of buoyant and flexible aquatic
688 vegetation. *Limnology and Oceanography*, 56(6), 2003-2017.
689 <https://doi.org/10.4319/lo.2011.56.6.2003>
690

691 Merritt, D. M., & Wohl, E. E. (2002). Processes Governing Hydrochory along Rivers : Hydraulics,
692 Hydrology, and Dispersal Phenology. *Ecological Applications*, 12(4), 1071-1087. JSTOR.
693 <https://doi.org/10.2307/3061037>
694

695 Nepf, H. M. (2012). Hydrodynamics of vegetated channels. *Journal of Hydraulic Research*, 50(3),
696 262-279. <https://doi.org/10.1080/00221686.2012.696559>
697

698 Nilsson, C., Brown, R. L., Jansson, R., & Merritt, D. M. (2010). The role of hydrochory in
699 structuring riparian and wetland vegetation. *Biological Reviews of the Cambridge Philosophical*
700 *Society*, 85(4), 837-858. <https://doi.org/10.1111/j.1469-185X.2010.00129.x>
701

702 Nilsson, C., Gardfjell, M., & Grelsson, G. (1991). Importance of hydrochory in structuring plant
703 communities along rivers. *Canadian Journal of Botany*, 69(12), 2631–2633.
704 <https://doi.org/10.1139/b91-328>
705

706 Palmer, M. R., Nepf, H. M., Pettersson, T. J. R., & Ackerman, J. D. (2004). Observations of particle
707 capture on a cylindrical collector : Implications for particle accumulation and removal in aquatic
708 systems. *Limnology and Oceanography*, 49(1), 76-85. <https://doi.org/10.4319/lo.2004.49.1.0076>
709

710 Peruzzo, P., Defina, A., & Nepf, H. (2012). Capillary trapping of buoyant particles within regions of
711 emergent vegetation. *Water Resources Research*, 48(7). <https://doi.org/10.1029/2012WR011944>
712

713 Peruzzo, P., Pietro Viero, D., & Defina, A. (2016). A semi-empirical model to predict the probability
714 of capture of buoyant particles by a cylindrical collector through capillarity. *Advances in Water*
715 *Resources*, 97, 168-174. <https://doi.org/10.1016/j.advwatres.2016.09.006>
716

717 Petit, S., Boursault, A., Guilloux, M., Munier-Jolain, N., & Reboud, X. (2011). Weeds in
718 agricultural landscapes. A review. *Agronomy for Sustainable Development*, 31(2), 309–317.
719 <https://doi.org/10.1051/agro/2010020>
720

721 R Core Team (2017). *R: A language and environment for statistical computing*. R Foundation for
722 Statistical Computing, Vienna, Austria. URL: <http://www.R-project.org>.
723

724 Ridley, H. N. (1930). *The Dispersal Of Plants Throughout The World* (L. Reeve & Co, LTD.).
725 <http://archive.org/details/TheDispersalOfPlantsThroughoutTheWorld>
726

727 Riis, T., & Sand-Jensen, K. (2006). Dispersal of plant fragments in small streams. *Freshwater*
728 *Biology*, 51(2), 274-286. <https://doi.org/10.1111/j.1365-2427.2005.01496.x>
729

730 Rubol, S., Ling, B., & Battiato, I. (2018). Universal scaling-law for flow resistance over canopies
731 with complex morphology. *Scientific Reports*, 8(1), 1-15. [https://doi.org/10.1038/s41598-018-](https://doi.org/10.1038/s41598-018-22346-1)
732 [22346-1](https://doi.org/10.1038/s41598-018-22346-1)

733

734 Rudi, G. (2019). Modélisation et analyse de services éco-hydrauliques des réseaux de canaux et
735 fossés des agrosystèmes méditerranéens [PhD Thesis]. Montpellier SupAgro, Montpellier, France.

736

737 Rudi, G., Bailly, J.-S., Belaud, G., Dages, C., Lagacherie, P., & Vinatier, F. (2020).
738 Multifunctionality of agricultural channel vegetation: A review based on community functional
739 parameters and properties to support ecosystem function modeling. *Ecohydrology & Hydrobiology*,
740 20(3), 397-412. <https://doi.org/10.1016/j.ecohyd.2020.03.004>

741

742 Rudi, G., Bailly, J.-S., Belaud, G., & Vinatier, F. (2018). Characterization of the long-distance
743 dispersal of Johnsongrass (*Sorghum halepense*) in a vegetated irrigation channel. *River Research
744 and Applications*, 34(9), 1219-1228. <https://doi.org/10.1002/rra.3356>

745

746 Rudi, G., Belaud, G., Troiano, S., Bailly, J. S., & Vinatier, F. (2020). Experimental dataset on seed
747 retention rates in a vegetated cover [Data set]. Zenodo. <http://doi.org/10.5281/zenodo.3947814>

748

749 Soomers, H., Winkel, D. N., Du, Y., & Wassen, M. J. (2010). The dispersal and deposition of
750 hydrochorous plant seeds in drainage ditches. *Freshwater Biology*, 55(10), 2032-2046.
751 <https://doi.org/10.1111/j.1365-2427.2010.02460.x>

752

753 Uva, R. H., Neal, J. C., & Ditomaso, J. M. (1997). *Weeds of the Northeast*. Ithaca, NY: Cornell
754 University Press.

755

756 Van Dijk, W. F. A., Van Ruijven, J., Berendse, F., & De Snoo, G. R. (2014). The effectiveness of
757 ditch banks as dispersal corridor for plants in agricultural landscapes depends on species' dispersal
758 traits. *Biological Conservation*, 171, 91–98. <https://doi.org/10.1016/j.biocon.2014.01.006>

759

760 Vella, D., & Mahadevan, L. (2005). The « Cheerios effect ». *American Journal of Physics*, 73(9),
761 817–825. <https://doi.org/10.1119/1.1898523>

762

763 Vinatier, F., Bailly, J.-S., & Belaud, G. (2017). From 3D grassy vegetation point cloud to hydraulic
764 resistance: Application to close-range estimation of Manning coefficients for intermittent open
765 channels. *Ecohydrology*, 10(8), e1885. <https://doi.org/10.1002/eco.1885>

766

767 Vinatier, F., Dollinger, J., Rudi, G., Feurer, D., Belaud, G., & Bailly, J.-S. (2018). The Use of
768 Photogrammetry to Construct Time Series of Vegetation Permeability to Water and Seed Transport
769 in Agricultural Waterways. *Remote Sensing*, 10(12), 2050. <https://doi.org/10.3390/rs10122050>
770

771 Vogel, S. (1996). *Life in Moving Fluids : The physical biology of flow* (Princeton University Press).
772 <https://press.princeton.edu/books/paperback/9780691026169/life-in-moving-fluids>
773

774 White, B. L., & Nepf, H. M. (2003). Scalar transport in random cylinder arrays at moderate
775 Reynolds number. *Journal of Fluid Mechanics*, 487, 43-79.
776 <https://doi.org/10.1017/S0022112003004579>
777
778

779 **TABLES**

780

781 **Table 1: Characteristics of the studied artificial plants.** The ramification number was based on
782 the methodology detailed in Godin and Caraglio (1998).

783

Variable	<i>Isolepsis sp.</i>	<i>Thuja sp.</i>	<i>Buxus sp.</i>
Standing length (cm)	63	30	20
Ramification number	0	1	2
Number of branching stems	0	30	11
Volume (cm ³)	241	230	147
Collar diameter (mm)	6	3	3
Leaf number	8	30	15
Projected surface area on horizontal plane (cm ²)	162	40	52
Cumulative leaf surface area (cm ²)	465	276	197

784 **Table 2: Summary of the experimental design.** SP represents the species, Q the discharge, D the
 785 density of plants by panels of 0.66*0.6 m and NB is the number of concrete panels filled with
 786 vegetation.
 787

SP	Q (in L.s ⁻¹)	D	Density per m ²	NB
First experiment				
<i>Isolepis</i> sp.	10-25-40	0-144	0-361.9	2
<i>Buxus</i> sp.	10-20	0-36	0-90.5	2
<i>Thuja</i> sp.	10-20-30	0-96	0-241.3	2
Second experiment				
<i>Isolepis</i> sp.	10	36	90.5	1, 2, 4, 6, 8
	25	60	150.8	1, 2, 4, 6, 8
	40	60	150.8	1, 2, 4, 6, 8
<i>Buxus</i> sp.	10	9	22.6	1, 2, 4, 6, 8
	20	9	22.6	1, 2, 4, 6, 8
<i>Thuja</i> sp.	10	12	30.2	1, 2, 3, 4, 6, 8
	20	24	60.3	1, 2, 3, 4, 6, 8

788

789 **Table 3: Effect of discharge (Q), density (D), species (SP), and interactions between density**
 790 **(D) and species (SP) on the rates of seed capture in a generalized linear model (glm) with a**
 791 **binomial error distribution. Density and discharge were used as the continuous variables, and**
 792 **species was used as the categorical variable. The P value indicates the significance of the model.**
 793

	d.f.	Deviance (Chi²- value)	Residual d.f.	Residual deviance	P value
Q	1	654.4	253	7047.3	< 0.001
D	1	3708.3	252	3339.0	< 0.001
SP	2	718.16	250	2620.8	< 0.001
D x SP	2	440.5	248	2180.3	< 0.001

794 **Table 4: Parameters fitted to the sigmoid curves from Equation 2.** *Q* is the discharge, *D*₅₀ the
 795 density needed to reach 50% seed retention, and *Slope* the slope of the linear relation between the
 796 density (*D*) and the seed retention rate (*R_r*).
 797

Studied plant	Q (in L.s ⁻¹)	<i>D</i> ₅₀	Slope	R ²
<i>Isolepis</i> sp.	10	43***	0.04***	0.86
	25	73***	0.03***	0.82
	40	91***	0.03***	0.88
<i>Buxus</i> sp.	10	6***	0.33***	0.90
	20	12***	0.24***	0.95
<i>Thuja</i> sp.	10	8***	0.28***	0.92
	20	20***	0.11***	0.85
	30	55***	0.04***	0.91

798 Significance codes of each parameter of the sigmoid curve fitted using non-least squares:
 799 '***' 0.001 '**' 0.01 '*' 0.05 '.' 0.1 ' ' 1

800

801 **Table 5: Presentation of the results of the fitted generic formula across various $Metrics_{veg}$**
 802 **and \mathfrak{R} values.**
 803

$Metrics_{veg}$	$\mathfrak{R} \times 10^{-5}$		
	R^2	RMSE	a
Scene representing real plant arrangements (“scene” method)			
Total vegetation ratio (Metrics 1)	0.24	0.255	3.678
Emergent vegetation ratio (Metrics 2)	0.18	0.279	3.669
Submerged vegetation ratio (Metrics 3)	0.77	0.126	0.961
Surface vegetation ratio (Metrics 4)	0.90	0.083	0.464
Product of the projected area of individual plants by plant densities (“product” method)			
Total vegetation ratio (Metrics 1)	0.12	0.321	11.55
Emergent vegetation ratio (Metrics 2)	0.08	0.339	14.95
Submerged vegetation ratio (Metrics 3)	0.49	0.205	1.448
Surface vegetation ratio (Metrics 4)	0.58	0.178	0.654

804 **Table 6: Estimation of the R^2 and RMSE of the best fitted generic formula for the three**
805 **studied plants.**

806

SP	Whole dataset	
	R^2	RMSE
<i>Buxus</i> sp.	0.83	0.26
<i>Isolepis</i> sp.	0.90	0.22
<i>Thuja</i> sp.	0.91	0.21

807